Power System Reliability Assessment Under Electric Vehicle and Photovoltaic Uncertainty

Jitendra Thapa, *Student Member, IEEE*, Joshua Olowolaju, *Student Member, IEEE*, Mohammed Benidris, *Senior Member, IEEE*, and Hanif Livani, *Senior Member, IEEE*

***Abstract*—In recent years, the adoption of electric vehicles (EVs) and variable energy resources such as photovoltaic (PV) has increased with the desire to reduce reliance on fossil fuels, decrease emissions, and promote sustainable energy. However, the increasing adoption of EVs and PVs has introduced unprecedented challenges to the reliability of power systems. The challenge lies in the inherent intermittency associated with solar generation and the uncertainty introduced by the charging load of EVs on the demand side of power grids. Therefore, it is indispensable from the perspective of power system operation and planning to consider the uncertainties associated with the output power of these resources in the reliability assessment framework. This paper develops an electric vehicle load model considering diverse charging station locations, EV types, and drivers' behavior. Also, the proposed method integrates the uncertainty of PV generation through interval prediction utilizing the K-Nearest Neighbors regressor. A sequential Monte Carlo simulation is used to analyze the impact of PV interval (forecasted lower and upper generation profile), EV load (hourly and peak), line failures, and demographic characteristics associated with EV on power system reliability. The reliability assessment is extended to sensitivity analysis and evaluation of the impact of EV loads and PV generation profiles on the capacity value of PV generators with different capacities, utilizing the Discrete Convolution approach. The proposed approach is demonstrated on the IEEE Reliability Test System and the results show the effectiveness of the proposed approach in determining the reliability of the power system by explicitly accommodating PV uncertainties and the intricacies of EVs.**

***Index Terms*—Composite reliability, electric vehicle, photovoltaic, uncertainty.**

I. Introduction

TRADITIONAL electric power systems are designed based on large central stations and passive, predictable, and stationary loads. However, this paradigm has been challenged by the large integration of variable energy resources (VERs) and the increasing penetration of electric vehicles (EVs). For instance, the proportion of wind and solar energy in the U.S. power grid is forecasted to increase from 1% in 2008 to 16% in 2023 [1]. The inherent variability associated with VERs can cause fluctuations in power generation, consequently impacting the reliability of the entire system. Additionally, the U.S. has established an ambitious goal, aiming for EVs to constitute 50% of total vehicle sales by 2030 [2]. The charging behavior of EVs introduces additional variability and uncertainty (both amount and location of EV charging) to the demand side, which also impacts power system reliability. With the sharp increase in the penetration of PVs and EVs, power grids will inevitably face cumulative consequences of integrating PV systems and EVs [3]. Several studies have explored the individual impacts of PVs and EVs [4]–[6]. However, there is a limited number of studies examining their combined effects on the reliability of the power grid. Thus, it has become indispensable to evaluate power system reliability considering the uncertainty of EV charging and PV power generation.

Composite power system reliability methods are primarily classified into analytical methods and Monte Carlo simulations (MCS) [7]. Analytical methods can provide an exact reliability index. However, they suffer from the curse of dimensionality [8] when assessing the reliability of practical-size systems and therefore, are less preferred. On the other hand, MCS methods, including sequential and non-sequential, provide greater flexibility in modeling uncertainties [9]–[11] and are scalable. However, they are time-consuming. Both analytical and MCS-based methods have been implemented in the literature to conduct power system reliability under PV and EV penetrations. In [12], the reliability of integrated transportation and electrical power system has been investigated by developing the model of a bidirectional EV charging station. In [13]–[15], the effect of EVs on power system load profile along with the improvement of power system reliability has been investigated. The impact of EVs using battery exchange mode on power system reliability has been explored in [16]. The work in [17] has proposed metrics to assess the influence of EVs on the reliability of the power grid using sequential MCS.

The impact of VERs on power system reliability has been extensively studied. For example, the impact of correlations between wind speed, solar irradiance, and load curve on composite power system reliability has been investigated in [18]. A combined reliability assessment and risk analysis framework have been developed to evaluate the effect of wind and solar integration on the grid [19]. The impact of wind power uncertainty on power system reliability has been studied in [20] along with the development of the wind power interval forecasting model. In addition, a Bayesian estimation approach has been used in estimating the parameters of the wind power point prediction model. An analytical method has been implemented to evaluate the reliability of the power system considering PV and energy storage in [21]. In [22], the capacity outage probability and frequency table (COPAFT) has been used to model the PV system for reliability assessment along with the sensitivity analysis of PV location on power

Jitendra Thapa and Mohammed Benidris are with the Department of Electrical and Computer Engineering, Michigan State University, East Lansing, MI 48824, USA, emails: thapajit@msu.edu and benidris@msu.edu

Joshua Olowolaju and Hanif Livani are with the Department of Electrical and Biomedical Engineering, University of Nevada, Reno, Reno, NV 89557 USA, emails: jolowolaju@nevada.unr.edu and hlivani@unr.edu

system reliability. In [23], an analytical-based reliability evaluation approach has been proposed considering the integration of renewable and non-renewable distributed generations with plug-in hybrid EVs.

The combined impact of EVs and renewable energy sources like PV on power system reliability considering their uncertainty is crucial to develop a practical basis for their integration into existing power systems. Also, most of the existing works have been focused on determining the point value of the reliability index. However, the computation of the reliability range is important, as it provides the system operator flexibility in conducting tasks related to planning for the integration of renewable sources, scheduling power, and executing dispatch operations. Moreover, as the penetration of PV increases, it is essential to evaluate their capacity value under different loading conditions (with and without EV) and determine their range considering the forecasted PV interval.

To address this research gap, this paper develops a reliability evaluation methodology designed to meticulously account for the uncertainties inherent in renewable generation, particularly photovoltaic (PV) power, while simultaneously incorporating the charging load imposed by EVs. This article advances our work presented in [24] by investigating the impact of peak load on power system reliability (with and without line failure) and the impact of different loading conditions and PV generation profiles on the capacity values of PV. A PV power point forecasting model is developed using a K-Nearest Neighbors (kNN) algorithm along with successive interval forecasting. The PV power interval prediction is conducted for one year to make it suitable for its integration for power system reliability assessment. The EV load model is constructed considering 30,000 EVs with different energy consumption per mile and 30 miles as an average daily driving distance along with consideration of the different locations of charging stations (i.e., residential and public charging stations). A load demand model, superimposing IEEE-Reliability Test System (IEEE RTS) system load and EV load, is constructed. Finally, the sequential Monte Carlo simulation is utilized to determine the range of reliability index of the IEEE RTS integrating the probabilistic prediction model of PV power and the developed EV load. The range of power system reliability indices is calculated by taking interval forecasting of PV power into consideration. Furthermore, the impact of different levels of EV penetration is also investigated.

The contribution of this article is summarized as follows:

- Developed a model for the hourly, daily, and weekly EV loads considering $30,000$ EVs with different classes, energy consumption, driver's behavior, and diverse charging locations.
- Developed a PV power interval prediction model that takes generation uncertainty into consideration and a real-world dataset collected from Henderson, Nevada is utilized. The interval prediction model facilitates the calculation of a range of reliability indices instead of a point index.
- Conducted extensive case studies investigating the impact of PV uncertainty, EV growth, generator's reliability parameters, and demographic characteristics associated with EV charging on power system reliability and capacity value of PV. The significance of such case studies is to provide future realization and prepare action plans to improve the reliability of power systems.

The remainder of the paper is organized as follows. Section II provides a description of the PV power interval forecasting model and EV load modeling. Section III provides a detailed explanation of the methodologies involved in this work. Section IV shows various test cases on the IEEE RTS reliability test system along with the determination of the range of reliability indices and investigation of EV's impact on power system reliability and capacity value of PV. Finally, Section V summarizes the paper and provides concluding remarks.

II. PV Power Interval Prediction Model, EV Load Modeling, and Critical Factors

A. PV Power Interval Prediction

The PV generation is associated with randomness and uncertainty because of their dependence on several environmental factors such as temperature and solar irradiance [25]. These uncertainties related to PV power are the major reasons for inaccurate point forecasting which in turn leads to ineffective generation scheduling decisions and risk analysis. Furthermore, a deterministic point forecast neglects those uncertainties which are detrimental from the perspective of safe and reliable operation of the power grid. Therefore, we develop an interval forecast model that considers uncertainties in PV power generation. The PV interval forecast provides the lower and upper bound of PV power at each hour of the forecasting interval with a certain degree of confidence. The significance of interval forecasting is that it facilitates the system operator to calculate the range of power system reliability. A real-world dataset collected from a PV-installed site (Henderson, Nevada) is used to obtain the PV profile for one year. Two scenarios with confidence degrees of 85%, and 95% are taken into consideration to forecast the PV interval and see the impact of the confidence interval on power system reliability.

A commonly used non-parametric technique known as K-Nearest Neighbors (kNN) is adopted in this work for time series point forecasting and ultimately constructing the interval. Consider a univariate time series data x=(x_1, x_2, $\cdots$, x_n) where 'n' is the number of data points. The kNN algorithm utilizes 'p' lagged values of the data points, X_t=(x_{t-1}, x_{t-2}, $\cdots$, x_{t-p}) as an input to forecast one step ahead $y_t = x_t$, as shown in Fig. 1. If there are 'n' data points, the number of input-output pairs is $n-p+1$. The estimation of an output for a corresponding test data point x_{ts} is based on the dissimilarity computed between the x_{ts} and all other x_{tr}, where, x_{tr} represents training input data points. The Euclidean distance is used as a measure of dissimilarity which is computed as follows:

$$dis(j) = ||x_{ts} - x_{tr}^{j}|| \; \forall j \in 1, \cdots, N_{tr} \tag{1}$$

where N_{tr} represents the number of training data points.

Based on the values of distance computed, the 'k' nearest neighbors x_{tr} of x_{ts} are identified and the predicted value is

This article has been accepted for publication in IEEE Transactions on Industry Applications. This is the author's version which has not been fully edited and content may change prior to final publication. Citation information: DOI 10.1109/TIA.2025.3532567

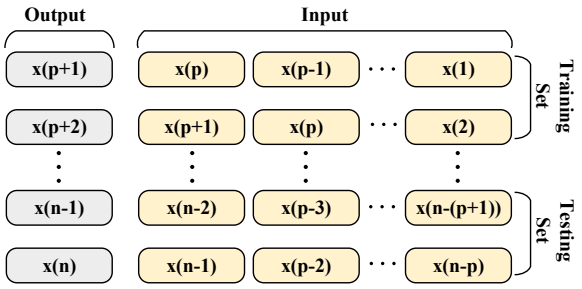

Fig. 1. Training and Testing Dataset of KNN

computed as the average of their corresponding y_{tr} values. In the event of a new prediction, the previous forecasted value is added to the input, and the consequent lagged values with the added forecasted value is utilized to predict the next value.

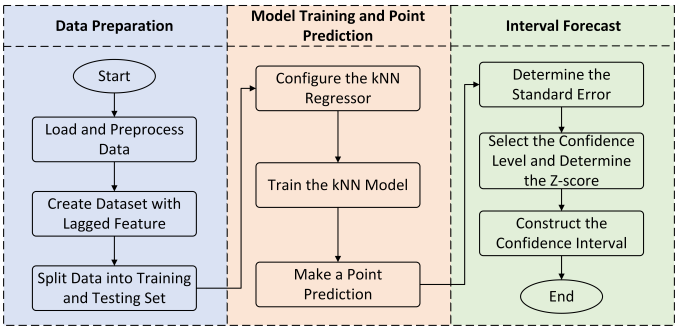

Fig. 2. Implementation of kNN Regressor for Interval Prediction

Fig. 2 represents the flowchart for the implementation of kNN regressor for interval prediction. The process starts with standardizing and preparing the labeled dataset with the lagged feature. As the PV profile dataset used in this paper is a univariate time series, lagged values of the variable to be forecasted have been used as features for kNN regression. The prepared dataset is split into the training and testing datasets. Before training, the kNN model is configured by selecting the appropriate number of neighbors (k) and a suitable distance metric. In this study, a distance metric called Euclidean distance is considered to find the nearest neighbors. The kNN regressor model is trained to predict the target value based on the nearest neighbors in the feature space (lagged values). Utilizing the predicted target values, the standard error (SE), which measures the variability and uncertainty in the forecast, is estimated. Next, the confidence level for the interval forecast is determined and the corresponding z-score is chosen. Finally, the point forecast, SE, and z-score are utilized to determine the interval forecast. The prediction interval evaluates the likelihood that PV generation will fall within a range of values for a certain proportion of instances. This interval is derived from the standard error of measurement. In this section, we report the outcome for a 95% prediction interval and validate our forecast by confirming that the actual value falls within the interval range 95% of the time. The power output of PV was predicted utilizing an 85% and a 95% prediction interval. Test analysis was conducted over the entire 8,760 hours for a 95% prediction interval to assess the precision of the interval forecast model. The evaluation indicated a 94.3% accuracy rate, demonstrating a strong correlation between the forecasted and actual values. The forecast interval areas for a 24-hour timeframe are depicted in Fig. 3. Prediction interval enables consideration of the PV power output variability.

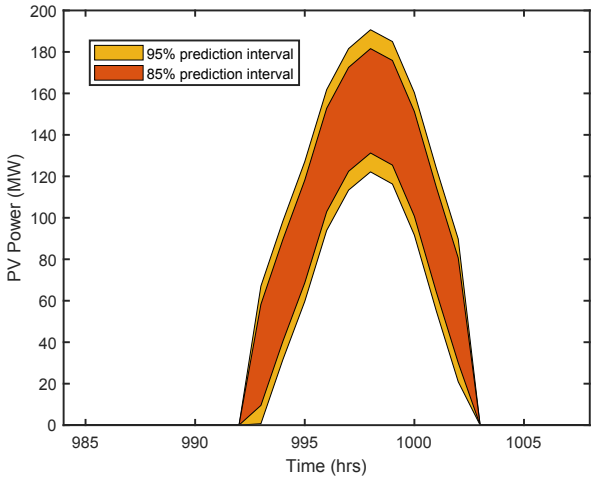

Fig. 3. PV Power Output Interval Prediction for 24 hours

B. Construction of EV Load Model

It is imperative to have an appropriate model for EV loads, which can be superimposed with the system load to evaluate the effect of charging demand on the reliability of the power system. In this research, we incorporate $30,000$ different types of EVs from [26], as shown in Table I, along with their corresponding consumption per unit distance. The average daily driving distance of 30 miles is assumed. The proportion of daily EV charging load in the residential and public charging stations is considered as 60 to 40 percent. Based on these numbers, the peak load for the residential and public charging stations is 199 MW and 132 MW. The EV load profile developed in [26], along with the hourly, daily, and weekly load demand for EV charging, is adopted in this study. Factors such as driver's behavior, location (residential and public), and time (weekdays and weekends) are taken into consideration. The EV load profile is constructed by manipulating the hourly (weekdays and weekend), daily, and weekly load profile shown in Fig. 4(a), Fig. 4(b), Fig. 5(a), and Fig. 5(b) respectively. These loads are expressed as percentages of daily, weekly, and annual peak loads respectively.

TABLE I
EVS CHARGING CONSUMPTION

EV Class	Number	KWh/mile	Average Daily Driving (mile)	Daily Consumption (MWh)
Sedan	18255	0.3225	30	176.62
Mid-Sedan	3582	0.3605	30	38.74
Mid-SUV	3930	0.4375	30	51.58
Full-SUV	4233	0.5075	30	64.48

1) Hourly EV Load: Fig. 4(a) and Fig. 4(b) represent the hourly EV charging load profile of EV expressed in percentage of daily peak load. The hourly load profiles of EV charging loads are constructed based on the data provided in [27]. From

This article has been accepted for publication in IEEE Transactions on Industry Applications. This is the author's version which has not been fully edited and content may change prior to final publication. Citation information: DOI 10.1109/TIA.2025.3532567

[27], the charging patterns in residential during the weekdays and weekends are different whereas the difference in charging patterns is negligible for public charging stations as illustrated in Fig. 4(a) and Fig. 4(b).

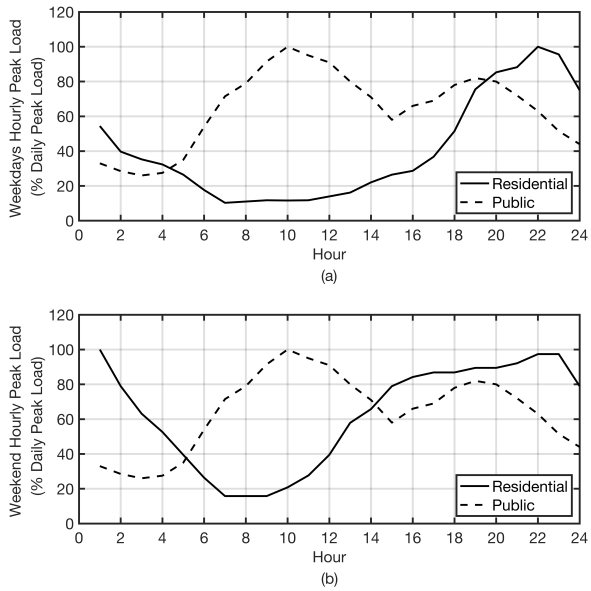

Fig. 4. EV Load Profile (a) Hourly Load (Weekdays) (b) Hourly Load (Weekend)

2) Daily EV Peak Load: Fig. 5(a) illustrates the daily charging peak load of EV expressed in percentage of weekly loads. The term daily peak load refers to the highest aggregate power demand from all connected EVs over 24 hours. User preferences and behavior, such as charging during off-peak hours or utilizing smart charging systems, can influence the distribution of the daily peak load. In this work, we adopt the data provided in [28] which has reported different values of peak loads during the weekdays and weekends, to construct the daily peak load profile of EV.

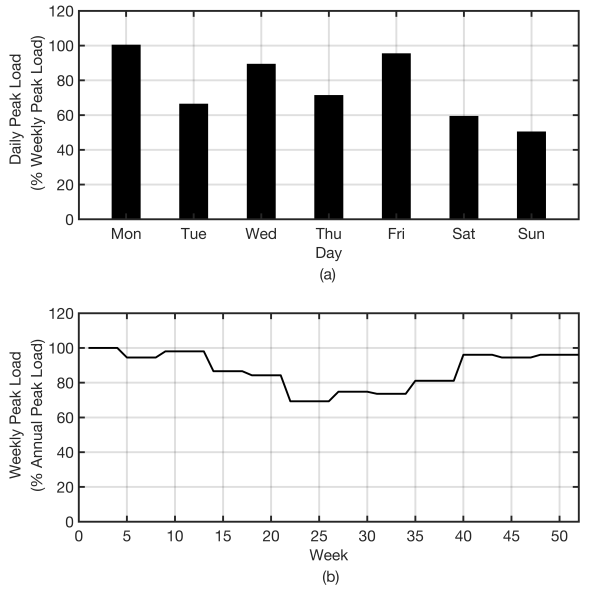

Fig. 5. EV Load Profile (a) Daily Load (b) Weekly Load

3) Weekly EV Peak Load: Fig. 5(b) represents the weekly peak load expressed in percentage of annual peak load. The monthly peak load provided in [29] is utilized for four weeks of the corresponding month. In each quarter, the peak of the third month is employed to derive the peak of five weeks rather than four, so as to compensate for the number of days dissimilarity between the duration of a month and the duration of four weeks.

C. Critical Factors

The reliability of the power system is influenced by a range of critical factors, including the load dynamics, characteristics of system components, line constraints, and consumer behaviors. Several case studies in Section IV are performed revolving around the following critical factors.

- Consumer behavior and Load Dynamics: Consumers play a major role in changing the dynamics of the load profile and demand patterns. For instance, the capacity and timing of EV charging can significantly impact load profiles. If a large number of EVs are charged simultaneously during peak hours, it can strain the system and reduce reliability.
- Line constraints: Line constraints help ensure that transmission lines do not exceed their operational limits, which could lead to overheating and potential damage. By adhering to these constraints, the system avoids line failures that could disrupt power delivery and compromise reliability.
- Characteristics of system components: Factors such as mean time to failure (MTTF) and mean time to repair (MTTR) measures the expected operational time before a generator fails and the time required to repair a generator after it fails, respectively. If generators have a large MTTF and small MTTR, the power system experiences fewer outages, leading to increased reliability.

III. Methodologies

A. Network Modeling and Optimization Problem Formulation

Composite power system reliability assessment, which involves heavy computation, requires a suitable DC power flow model to overcome the issues of computation burden [30]. Furthermore, DC power flow models are sufficiently accurate for composite power system reliability evaluation. Therefore, a DC power flow model [31] combined with constraints of the power balance equation, generation capacity limits, and transmission line capacity is considered to formulate a linear programming problem with an objective of minimizing the amount of load curtailment. The assumptions involved with the usage of DC power flow along with their limitations are as follows:

- Voltage Magnitudes are constant: The model assumes that voltage magnitudes are fixed and do not vary with changes in power flow. This assumption simplifies the equations but overlooks the impact of voltage fluctuations on system reliability.
- Small Angle Approximation: The DC power flow model assumes that the voltage angle differences between buses

are small. This allows the use of the approximation $sin(\theta) \approx \theta$ and $cos(\theta) \approx 1$, which linearizes the power flow equation.

- Neglecting Reactive Power: Reactive power is not considered in the DC power flow model. The model does not account for the requirement of reactive power for maintaining voltage levels and also ignores the constraints associated with the reactive power of generator and flows.
- Lossless Transmission lines: The model assumes that transmission lines are lossless, meaning that line losses are neglected. This assumption simplifies the power flow equations but can lead to inaccuracies, especially in systems with significant line losses.

Consider a transmission network with N_B buses and N_T transmission lines. Equation (2) represents the objective function to minimize the load curtailment C_i at each bus, where, C_i is the difference between the generation and load at each bus.

$$\min \left\{ \sum_{i=1}^{N_B} C_i \right\} \tag{2}$$

subject to:

$$B\delta + G + C = L \tag{3}$$

$$B_T A\delta \leq T^{max} \tag{4}$$

$$-B_T A\delta \leq T^{max} \tag{5}$$

$$G^{min} \leq G \leq G^{max} \tag{6}$$

$$0 \leq C \leq L \tag{7}$$

$$-\pi \leq \delta \leq \pi \tag{8}$$

The equality constraint (3) describes the power balance constraint at each bus, where $B_{(N_B \times N_B)}$ is a bus susceptance matrix, $\delta_{(N_B \times 1)}$ represents vector of angle of bus voltages, $G_{(N_B \times 1)}$ represents the vector of generator's power at each bus, $L_{(N_B \times 1)}$ and $C_{(N_B \times 1)}$ are the vectors of the load and load curtailment at each bus respectively. The inequality constraints presented in equations (4) and (5) limit the transmission line capacity, where $B_{T\,(N_T \times N_T)}$ is a transmission line susceptance matrix, $A_{(N_B \times N_B)}$ is the element-node incidence matrix, $T^{max}_{(N_T \times 1)}$ represents the maximum transmission line capacity limit. Equation (6) represents the generator's power constraint, where G^{min} and G^{max} are both vectors of size $(N_B \times 1)$ representing lower and upper bound of generator power at each bus. As the load curtailment C_i at each bus is positive and cannot be more than the respective load L_i, C_i is bounded between zero and the load of the respective bus as given by the equation (7). The inequality constraint given in (8) represents the bounds for bus voltage angles.

B. Sequential Monte Carlo Simulation

In this paper, the Sequential Monte Carlo (SMC) approach is utilized to simulate a sequential time evolution of the system state and assess the power system reliability. Sequential simulation approaches can provide additional time-related indices such as duration and frequency of load loss. SMC approaches are designed to handle sequential and time-dependent aspects of power system reliability analysis. In contrast to the non-sequential methods, SMC can model chains of events and their probabilistic impacts on system reliability, offering insights into how a sequence of failures or disturbances propagate through the system. Moreover, SMC simulation can efficiently handle large-scale systems and high-dimensional input space whereas analytical methods suffer from the curse of dimensionality with the large-scale system. Furthermore, SMC captures uncertainties and variabilities as these are probabilistic methods in comparison to the deterministic approaches and analytical methods.

There are two approaches for sequential MCS: (i) the fixed interval method, and (ii) the next event method. In this work, the next event method is adopted where the time is advanced to the occurrence of the next event [32]. Fig. 6 illustrates the overall flowchart of the proposed approach to evaluate the reliability of the power system under the penetration of EV and PV using Sequential MCS. The overall flowchart summarizes the steps involved in EV load modeling, PV interval forecast, and simulation under the next event method of sequential MCS. The simulation is carried out for 100 years as the considered duration is sufficient for all the scenarios to converge.

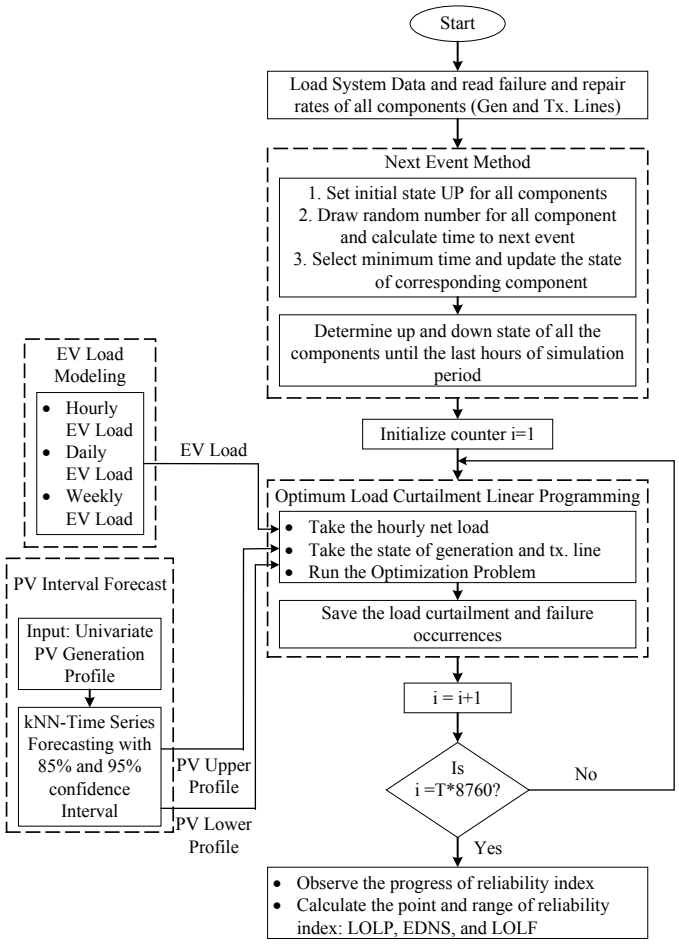

Fig. 6. Overall Flowchart for the Proposed Approach

Reliability indices such as loss of load probability (LOLP), expected demand not supplied (EDNS), and loss of load fre-

quency (LOLF) are evaluated. The description and expression to determine the reliability indices are described in [24].

C. Discrete Convolution to Evaluate Capacity Value of PV

The capacity value represents the additional load that can be incorporated into the system following the installation of a generator while preserving the original system's reliability. The capacity value of an added generator is a measure of its contribution to maintaining the adequacy of generation to meet the load demand. As PV generation is dependent upon environmental conditions such as temperature and irradiance, they are not controllable like conventional generators and therefore, it is necessary to evaluate their capacity value. In this study, the discrete convolution technique is used to compute the capacity value of the added PV generator. The discrete convolution technique involves constructing probability and frequency distribution of random variables representing the total system generation and the total system load. Particularly, a Capacity Outage Probability and Frequency Table (COPAFT) is constructed which represents the analytical reliability model. A recursive unit addition algorithm implemented in this work updates the COPAFT through discrete convolution of probability and frequency distribution of the new unit with the existing system [33]. The load model is constructed utilizing the hourly load profile in the form of the triplet $(L_j,\ P(L \geq L_j),\ F(L \geq L_j)$, where, L_j represents the load, $P(L \geq L_j)$ represents the probability of load greater than L_j, and $F(L \geq L_j)$ represents the cumulative frequency for load L_j. Finally, the generation reserve margin model is constructed utilizing the generation and load model to compute the generation adequacy indices. In this study, the capacity value of PV is computed based on the LOLP. The steps for determining the capacity value is as follows:

- Initially, the LOLP for the existing system is computed without considering the presence of PV, which acts as a target LOLP after the addition of PV.
- The net load of the system is computed considering the time series PV generation profile as a negative load. The LOLP is computed again, which is expected to be lower than the LOLP computed in Step 1 due to load reduction.
- The net load profile is incremented by a ΔL until the target LOLP is achieved. The sum of ΔL represents the capacity value of the added PV.

IV. Case Studies and Results

The IEEE RTS is used to determine and compare reliability indices for several scenarios with PVs and EVs. The IEEE RTS consists of 24 buses, 38 transmission lines, and 32 generators with their capacity ranging from 12 MW to 400 MW. All the data required for reliability analysis such as generators' capacity, loads (hourly, daily, weekly), and transmission line limits, failure and repair rate of components are obtained from [34]. For the analysis, the yearly generation profile of three Pv systems with a maximum capacity of 200 MW, 200 MW, and 100 MW are aggregated and distributed across all the buses where loads are connected. The first case study involves the investigation of the impact of different confidence degrees of PV forecast on the composite reliability of power systems with a fixed base load of EV. The second case study determines the impact of different levels of EV penetration on power system reliability considering a fixed confidence degree of PV interval forecast. The third case study evaluates the reliability index under different peak load conditions with the addition of EV. The fourth case study evaluates the capacity value of PV and determines its sensitivity to different PV generation profiles and loading conditions. The final case study investigates the sensitivity of reliability metrics to change in generator's availability.

A. Composite Reliability Evaluation for Different Confidence Degrees of PV Interval Forecast

The consideration of interval forecast of renewable generation for reliability assessment is to consider their uncertainty and variability. Operational reliability assessment using point forecast provides a fixed set of generation scheduling, which does not provide flexibility to the system operators. The significance of integrating interval forecast for reliability analysis are: (a) it considers uncertainty, (b) it allows system operators to calculate the range of reliability indices, (c) it provides more flexibility in generation planning and scheduling for operational reliability.

In this case study, PV interval forecast with 85% and 95% confidence level is integrated with a fixed base load penetration of EV on the IEEE RTS. The sequential Monte Carlo simulation is used to calculate the LOLP, EDNS, and LOLF. Each of the reliability indices is calculated considering both the lower and upper limits of PV forecast and subsequently, the range of reliability indices is determined. Furthermore, the significance of this case study is to evaluate the impact of adding PV on power system reliability and compare it with the reliability of the original system with and without EV. Table-II illustrates the value of reliability metrics for different degrees of PV forecasting confidence interval. The result demonstrates that the original system without the integration of PV and EV is more reliable than a system with PV and EV. As the second scenario in Table-II involves only EV integration, the system is more stressed because of increasing load. The addition of PV increases the reliability of the system which can be seen from the scenarios of system with both EV and PV. In terms of magnitude, the generation profile of PV associated with the upper and lower limit of 95% confidence interval is the highest and lowest respectively in comparison to other considered scenarios. Therefore, among the PV considered scenarios, the most reliable system is observed when the upper limit at 95% confidence interval is taken as the generation profile for PV.

Fig. 7 illustrates the comparison of power system reliability before and after the integration of PV on the IEEE RTS with and without EV. The convergence of reliability metrics over the simulation period is shown for a specific case with 95% confidence interval of PV forecast. At the beginning of the simulation, the value of reliability metrics is larger compared to the value at the final stage of the simulation. However, as the simulation progresses, the indices converge to their true values. Furthermore, Fig. 7 provides clear visualization on the range

TABLE II
COMPARISON AND EVALUATION OF RANGE OF RELIABILITY INDICES FOR PV INTERVAL FORECAST WITH DIFFERENT CONFIDENCE INTERVAL

System	Confidence Degree (%)	LOLP	EDNS (MW/yr)	LOLF (Occ/yr)
IEEE-RTS	-	0.0013	0.151	1.99
IEEE-RTS with EV	-	0.0034	0.487	6.56
IEEE-RTS with EV & PV (Lower Limit)	95	0.0022	0.2981	6.21
	85	0.002	0.2591	5.78
IEEE-RTS with EV & PV (Upper Limit)	85	0.0016	0.2219	5.2
	95	0.0013	0.1601	4.9

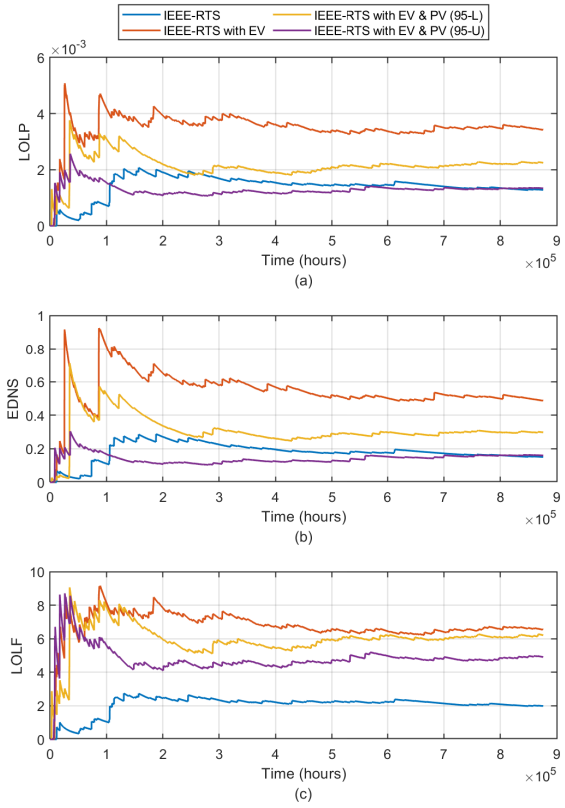

Fig. 7. Comparison of Reliability Indices for Different Degrees of PV Interval Forecast (a) Convergence of LOLP (b) Convergence of EDNS (c) Convergence of LOLF

of reliability index under penetration of EVs and PVs. Fig. 7 also illustrates that when the PV output takes the upper limit of 95% confidence interval, the system is able to retain the level of reliability (in terms of LOLP and EDNS) as in the case of original IEEE RTS with no PV and EV. The particular result gives an idea of the additional generation required to retain the reliability of the original system. The results presented in Table-II can also be validated through Fig. 7.

B. Composite Reliability Evaluation with Different Levels of EV Penetration and a Fixed Degree of PV Interval Forecast

1) EV Load Distributed Across all the Load Buses Based on their Proportion: In this case study, a composite reliability assessment of IEEE RTS is conducted considering its annual load profile in hourly granularity with different penetration levels of EV load. The PV interval forecast with the confidence degree of 95% is used for all scenarios. Furthermore, the penetration of EV load is increased with the step of 20% up to 100% to determine the impact of different levels of EV charging load on reliability. With such a case study, modern utilities can prepare for future scenarios of heavy penetration of EVs. Furthermore, utilities can plan for generation expansion, network reconfiguration, the addition of renewable, etc. in advance if such realization of future scenarios can be done early. A key benefit of this case study is that it establishes a foundation to determine the additional generation needed to retain the reliability of the system when the system load increases.

Table-III represents the annual reliability indices for different penetration levels of EV load. The result presented in Table-III illustrates that the system reliability decreases as the penetration level of EV increases. As the reliability metrics such as LOLP, EDNS, and LOLF are all related to loss of load or curtailments, the higher value indicates a less reliable system. Furthermore, the reliability indices computed with a lower interval limit of PV are higher compared to the values calculated with an upper interval limit. As the generation profile of PV associated with the upper limit of the interval forecast is larger compared to that of the lower limit, the system is more reliable when the upper limit is taken as the generation profile for PV. Furthermore, the values of LOLP and EDNS demonstrate significant differences between any two scenarios; however, the respective difference is not observed in the case of LOLF. As LOLF is just an indicator of the frequency of loss of load in a year, two scenarios with the same value of LOLF can have different amounts of curtailments per year. Therefore, it is imperative to observe either LOLP or EDNS combined with LOLF to analyze the reliability of the system.

2) EV Load Distributed Assuming Demographic Characteristics of Load Buses: In this case study, the EV load is distributed across all the load buses based on the demographic characteristics of each of these buses. Here, the term demographic characteristics is introduced to allocate higher EV charging tendency to some of the buses. Among 17 load buses in the IEEE RTS, load buses are categorized into four categories; Group_1 (1, 2, 5, 7, 8), Group_2 (3, 4, 6, 9, 10), Group_3 (13, 14, 15, 16), and Group_4 (18, 19, 20). The distribution of EV load in each group is 40%, 25%, 20%, and 15% respectively, which depicts the higher EV charging tendency of Group_1. The significance of this study is to determine the impact of demographic characteristics on power system reliability and compare the results with the scenario of EV load distributed based on the proportion of the bus's load. In this case study as well, the 95% PV interval forecast has been used for the purpose of analysis.

Table-IV represents the annual reliability indices for different penetration levels of EV load along with the distribution based on the assumed demographic characteristics of load buses. Comparing the results presented in Table-IV with Table-III, the system reliability index is found to be almost similar up to 60% increment in penetration of EV. However, the impact of EV load distribution based on the assumed demographic characteristic is significant when the EV penetration is increased by 80% and 100% of its base load.

TABLE III
EVALUATION OF RELIABILITY INDICES FOR DIFFERENT PENETRATION LEVELS OF EV
(EV LOAD DISTRIBUTED BASED ON THE PROPORTION OF LOAD BUS)

System	PV lower limit (95%)			PV upper limit (95%)		
	LOLP	EDNS (MW/yr)	LOLF (Occ/yr)	LOLP	EDNS (MW/yr)	LOLF (Occ/yr)
IEEE-RTS with EV	0.0022	0.2981	6.21	0.0013	0.1601	4.9
IEEE-RTS with 1.2*EV	0.0025	0.3178	7.27	0.0019	0.2398	6.84
IEEE-RTS with 1.4*EV	0.0031	0.4473	8.69	0.0024	0.3174	8.38
IEEE-RTS with 1.6*EV	0.0034	0.4614	10.23	0.0029	0.4411	10.12
IEEE-RTS with 1.8*EV	0.0038	0.599	11.82	0.0034	0.4779	10.76
IEEE-RTS with 2.0*EV	0.0047	0.745	12.99	0.0038	0.6067	12.63

TABLE IV
EVALUATION OF RELIABILITY INDICES FOR DIFFERENT PENETRATION LEVEL OF EV
(EV LOAD DISTRIBUTED ASSUMING DEMOGRAPHIC CHARACTERISTICS OF LOAD BUSES)

System	PV lower limit (95%)			PV upper limit (95%)		
	LOLP	EDNS (MW/yr)	LOLF (Occ/yr)	LOLP	EDNS (MW/yr)	LOLF (Occ/yr)
IEEE-RTS with EV	0.0021	0.3046	5.49	0.0011	0.1488	4.2
IEEE-RTS with 1.2*EV	0.0024	0.3248	6.94	0.002	0.2785	6.67
IEEE-RTS with 1.4*EV	0.003	0.4163	8.81	0.0026	0.3916	8.44
IEEE-RTS with 1.6*EV	0.0033	0.4698	10.2	0.003	0.4444	9.6
IEEE-RTS with 1.8*EV	0.0046	0.6754	13.01	0.0036	0.5225	12.86
IEEE-RTS with 2.0*EV	0.0055	0.8454	15.47	0.0045	0.6896	15.24

The reason behind the insignificant difference in the indices up to 60% increment in EV load can be attributed to the ability of the impacted transmission line to carry the incremented power. However, in the case of 80% and 100% EV load increment, the transmission line capacity is not sufficient to accommodate the increased power flows. In order to observe the impact of assumed demographic characteristics-based EV load distribution, the calculation of the local reliability index is imperative rather than the calculation of system reliability.

C. Impact of Peak Load on Reliability

In this case study, the annualized index is calculated to determine the impact of peak load under different penetration levels of EV. Also, the impact of line failure consideration on the composite power system reliability is determined as well. The possibility of line failure impact is more when calculating annualized indices as the peak load of a yearly load profile is considered for the analysis. During peak load, all the transmission lines need to carry the power to fulfill the demand. However, during light load, even the failure of a few lines can be compensated through the usage of other lines. Table V represents the annualized index for IEEE RTS with and without the consideration of line failure. The second column in the Table V provides the value of peak loads under different EV penetrations. Table V clearly illustrates that the reliability index calculated considering line failure is larger compared to that of analysis without considering line failure. The value of all the reliability index increases as the penetration level of EV increases which can be observed in Table V. The comparison of the second scenario with base EV load integration on IEEE RTS in Table V and Table-II shows that the annualized reliability index is significantly larger than the corresponding annual index.

D. Capacity Value Evaluation of PV Using Discrete Convolution

In this case study, the capacity value of PV with different capacities is computed under different loading conditions and PV generation profiles. Table VI presents the capacity value of PV with capacity ranging from 0 MW to 300 MW. The capacity values are in terms of the percentage of installed capacity. The predicted PV generation profile along with its lower and upper generation profiles are determined by scaling the corresponding profiles of 200 MW PV with 95% confidence interval. The influence of EV load is neglected and only the IEEE RTS system load is considered to observe the sole impact of PV generation profile on its capacity value. Table VI shows that the capacity values calculated based on the upper generation profile are higher in comparison to the capacity values calculated based on the predicted and lower generation profiles. The significance of this particular case study is to provide the range of capacity value of added PV to the system operator.

The capacity value of PV depends upon several factors but the key factor is the coincidence of PV generation profile with the electricity demand pattern. Controllable units, such as thermal and hydro units, can be adjusted and scheduled based on the load demand which assists in achieving high-capacity values for the respective units. However, variable renewable generators, such as PV and wind, depend upon environmental factors and their capacity value also depend on the correlation of their generation with the load. Table VII illustrates the difference in the capacity value of PV under different loading conditions. This case study is conducted based on the scaled upper PV generation profile of 200 MW with 95% confidence interval. The capacity value under column III in Table VII is calculated considering the base load of IEEE RTS whereas column IV is calculated after the addition of EV load in the

TABLE V
ANNUALIZED INDEX FOR IEEE RTS WITH AND WITHOUT LINE FAILURE

System	Peak Load (MW)	Without line failure			With line failure		
		LOLP	EDNS (MW/yr)	LOLF (Occ/yr)	LOLP	EDNS (MW/yr)	LOLF (Occ/yr)
IEEE RTS	2850	0.0834	14.0186	19.19	0.0992	19.2686	26.53
IEEE RTS with EV	3010	0.2519	34.6829	22.7	0.276	41.423	28.43
IEEE RTS with 1.2*EV	3053.4	0.2824	47.1747	27.18	0.317	57.8232	33.71
IEEE RTS with 1.4*EV	3096.8	0.315	59.644	29.05	0.3343	68.5134	33.6
IEEE RTS with 1.6*EV	3140.2	0.3388	76.6511	33.28	0.3498	83.7082	38.71
IEEE RTS with 1.8*EV	3183.6	0.3514	90.9122	38.44	0.3683	96.2372	44.37
IEEE RTS with 2*EV	3227	0.4198	106.206	44.84	0.4314	112.9503	49.01

TABLE VI
CAPACITY VALUE (% OF INSTALLED CAPACITY) UNDER DIFFERENT PV GENERATION PROFILE

Capacity (MW)	CV (%) based on Predicted PV profile	CV (%) based on Predicted Lower PV profile (95%)	CV (%) based on Predicted Upper PV profile (95%)
0	0	0	0
20	25	10	30
40	25	15	35
60	28.33	16.67	36.67
80	28.75	17.50	36.25
100	29	17	36
120	29.17	17.50	35.83
140	28.57	17.86	35.71
160	28.75	17.50	35.00
180	28.33	17.22	34.44
200	28.50	17.00	33.50
220	28.18	16.82	33.18
240	27.92	16.67	32.50
260	27.31	16.92	31.92
280	27.14	16.43	31.07
300	27.00	16.33	30.67

TABLE VII
CAPACITY VALUE (% OF INSTALLED CAPACITY) WITH AND WITHOUT EV LOAD

Capacity Factor	Capacity (MW)	CV (%) Based on LOLP (IEEE RTS load)	CV (%) Based on LOLP (IEEE RTS plus EV load)
0	0	0	0
0.1	20	30	35
0.2	40	35	35
0.3	60	36.667	35
0.4	80	36.250	35
0.5	100	36.000	34
0.6	120	35.833	33.333
0.7	140	35.714	32.143
0.8	160	35.000	31.875
0.9	180	34.444	31.111
1	200	33.500	30.000
1.1	220	33.182	29.545
1.2	240	32.500	28.750
1.3	260	31.923	28.077
1.4	280	31.071	27.500
1.5	300	30.667	26.667

base load of IEEE RTS. The penetration of EV load can shift the load profile of a system and can either increase or decrease the correlation between the generation profile of PV with the load profile. In almost all cases, the addition of EV load decreases the capacity value of the PV which is also shown through Table VII. The reduction in capacity value is attributed to the decrease in coincidence between the PV profile and resultant load profile due to the addition of EV load.

E. Sensitivity Analysis

In this case study, a sensitivity analysis is conducted to observe the impact of availability parameters of a generator on power system reliability. The MTTF of the largest generator, having a capacity of 400 MW and located at bus 21, is varied, and the corresponding reliability metrics are computed. Considering the ratio of base MTTF and MTTR as 1 per unit, the MTTF is varied such that the per unit value is changed from 0.5 to 1.5 per unit. Table VIII illustrates the sensitivity of all the reliability metrics to different values of availability of the largest generator. The result demonstrates that the decrease in per-unit values increases the downtime and reduces the system reliability, causing more load curtailment or requiring additional reserve resources. Conversely, increasing the per-unit values enhances the system's reliability and reduces load curtailment. This sensitivity analysis can identify critical components whose reliability has a disproportionate effect on overall system performance, guiding maintenance strategies, and investment decisions.

TABLE VIII
SENSITIVITY OF RELIABILITY METRICS TO CHANGE IN GENERATOR'S AVAILABILITY

Per Unit (Ratio of MTTF to MTTR)	LOLP	EDNS (MW/yr)	LOLF (Occ/yr)
1.5	0.0007	0.0639	3.29
1.4	0.0008	0.0707	3.56
1.3	0.0009	0.0839	3.82
1.2	0.001	0.1131	4.19
1.1	0.0011	0.1352	4.43
1	0.0013	0.1601	4.9
0.9	0.0016	0.2259	5.41
0.8	0.0018	0.2455	6.14
0.7	0.0019	0.2915	6.38
0.6	0.0021	0.2991	7.25
0.5	0.0024	0.35	8.24

V. CONCLUSION

The paper has conducted a comprehensive reliability analysis for a power system, considering uncertainties in photovoltaic (PV) power and the influence of electric vehicles (EVs). To assess the impact of uncertainty associated with PV power generation, a PV interval forecasting model was

developed using the K-Nearest Neighbors (kNN) algorithm. An hourly, daily, and weekly EV load models were developed considering different factors such as locations of charging stations, types of EVs, and drivers' behavior. Multiple case studies were conducted to determine the annual and annualized reliability indices under different penetrations of EV load along with the consideration of forecasted PV interval. Annual and annualized reliability indices were computed using Sequential Monte Carlo simulation (MCS) to determine the impact of PV interval, combined system load (hourly and peak), line failures, and demographic characteristics associated with EV. Furthermore, the study was extended to perform sensitivity analysis and determine the impact of different loading conditions and PV generation profiles on the capacity value of PVs with different capacities. The calculation of capacity value was based on loss of load probability (LOLP) and discrete convolution was utilized. The proposed approach was demonstrated in the IEEE Reliability Test System. The results demonstrated the effectiveness of the proposed approach to conduct a detailed reliability analysis under the consideration of uncertainties associated with the EV and PV.

ACKNOWLEDGEMENT

This work was supported in part by the U.S. National Science Foundation (NSF) under Grant NSF 1847578.

REFERENCES

[1] "Increasing renewables likely to reduce coal and natural gas generation over next two years," accessed: 2024-01-13. [Online]. Available: https://www.eia.gov/todayinenergy/detail.php?id=55239#

[2] "Electric Vehicle and Rural Transportation," accessed: 2023-12-25. [Online]. Available: https://www.transportation.gov/rural/ev

[3] A. Tavakoli, S. Saha, M. T. Arif, M. E. Haque, N. Mendis, and A. M. Oo, "Impacts of grid integration of solar pv and electric vehicle on grid stability, power quality and energy economics: A review," *IET Energy Systems Integration*, vol. 2, no. 3, pp. 243–260, 2020.

[4] J. de Hoog, V. Muenzel, D. C. Jayasuriya, T. Alpcan, M. Brazil, D. A. Thomas, I. Mareels, G. Dahlenburg, and R. Jegatheesan, "The importance of spatial distribution when analysing the impact of electric vehicles on voltage stability in distribution networks," *Energy Systems*, vol. 6, pp. 63–84, 2015.

[5] M. Mosadeghy, R. Yan, and T. K. Saha, "Impact of pv penetration level on the capacity value of south australian wind farms," *Renewable energy*, vol. 85, pp. 1135–1142, 2016.

[6] J. Mullan, D. Harries, T. Bräunl, and S. Whitely, "Modelling the impacts of electric vehicle recharging on the western australian electricity supply system," *Energy policy*, vol. 39, no. 7, pp. 4349–4359, 2011.

[7] F. Chen, F. Li, W. Feng, Z. Wei, H. Cui, and H. Liu, "Reliability assessment method of composite power system with wind farms and its application in capacity credit evaluation of wind farms," *Electric Power Systems Research*, vol. 166, pp. 73–82, 2019.

[8] A. M. L. da Silva, J. F. C. Castro, and R. A. González-Fernández, "Spinning reserve assessment under transmission constraints based on cross-entropy method," *IEEE Transactions on Power Systems*, vol. 31, no. 2, pp. 1624–1632, 2015.

[9] S. Conti and S. A. Rizzo, "Monte carlo simulation by using a systematic approach to assess distribution system reliability considering intentional islanding," *IEEE Transactions on Power Delivery*, vol. 30, no. 1, pp. 64–73, 2014.

[10] H. Lei and C. Singh, "Non-sequential monte carlo simulation for cyber-induced dependent failures in composite power system reliability evaluation," *IEEE Transactions on Power Systems*, vol. 32, no. 2, pp. 1064–1072, 2016.

[11] L. Urbanucci and D. Testi, "Optimal integrated sizing and operation of a chp system with monte carlo risk analysis for long-term uncertainty in energy demands," *Energy conversion and management*, vol. 157, pp. 307–316, 2018.

[12] K. Hou, X. Xu, H. Jia, X. Yu, T. Jiang, K. Zhang, and B. Shu, "A reliability assessment approach for integrated transportation and electrical power systems incorporating electric vehicles," *IEEE Transactions on Smart Grid*, vol. 9, no. 1, pp. 88–100, 2016.

[13] C. D. White and K. M. Zhang, "Using vehicle-to-grid technology for frequency regulation and peak-load reduction," *Journal of Power Sources*, vol. 196, no. 8, pp. 3972–3980, 2011.

[14] W. Kempton and T. Kubo, "Electric-drive vehicles for peak power in japan," *Energy policy*, vol. 28, no. 1, pp. 9–18, 2000.

[15] J. Kiviluoma and P. Meibom, "Influence of wind power, plug-in electric vehicles, and heat storages on power system investments," *Energy*, vol. 35, no. 3, pp. 1244–1255, 2010.

[16] L. Cheng, Y. Chang, J. Lin, and C. Singh, "Power system reliability assessment with electric vehicle integration using battery exchange mode," *IEEE Transactions on Sustainable Energy*, vol. 4, no. 4, pp. 1034–1042, 2013.

[17] M. Kamruzzaman and M. Benidris, "Reliability-based metrics to quantify the maximum permissible load demand of electric vehicles," *IEEE Transactions on Industry Applications*, vol. 55, no. 4, pp. 3365–3375, 2019.

[18] Z. Qin, W. Li, and X. Xiong, "Incorporating multiple correlations among wind speeds, photovoltaic powers and bus loads in composite system reliability evaluation," *Applied energy*, vol. 110, pp. 285–294, 2013.

[19] I. Akhtar, S. Kirmani, and M. Jameel, "Reliability assessment of power system considering the impact of renewable energy sources integration into grid with advanced intelligent strategies," *IEEE Access*, vol. 9, pp. 32 485–32 497, 2021.

[20] X. Yang, Y. Yang, Y. Liu, and Z. Deng, "A reliability assessment approach for electric power systems considering wind power uncertainty," *IEEE Access*, vol. 8, pp. 12 467–12 478, 2020.

[21] L. H. Koh, W. Peng, K. J. Tseng, and G. ZhiYong, "Reliability evaluation of electric power systems with solar photovoltaic energy storage," in *2014 International Conference on Probabilistic Methods Applied to Power Systems (PMAPS)*, 2014, pp. 1–5.

[22] S. Sulaeman, M. Benidris, and J. Mitra, "Modeling and assessment of pv solar plants for composite system reliability considering radiation variability and component availability," in *2016 Power Systems Computation Conference (PSCC)*, 2016, pp. 1–8.

[23] A.-M. Hariri, H. Hashemi-Dezaki, and M. A. Hejazi, "A novel generalized analytical reliability assessment method of smart grids including renewable and non-renewable distributed generations and plug-in hybrid electric vehicles," *Reliability Engineering & System Safety*, vol. 196, p. 106746, 2020.

[24] J. Thapa, J. Olowolaju, H. Livani, and M. Benidris, "Composite power system reliability assessment considering uncertainty of electric vehicle charging and pv power generation," in *2023 IEEE Industry Applications Society Annual Meeting (IAS)*, 2023, pp. 1–7.

[25] Y. Han, N. Wang, M. Ma, H. Zhou, S. Dai, and H. Zhu, "A pv power interval forecasting based on seasonal model and nonparametric estimation algorithm," *Solar Energy*, vol. 184, pp. 515–526, 2019.

[26] M. Kamruzzaman, M. Benidris, and S. Elsaiah, "Effective load demand of electric vehicles in power system adequacy assessment," in *2018 IEEE International Conference on Probabilistic Methods Applied to Power Systems (PMAPS)*, 2018, pp. 1–5.

[27] U. DoE, "Evaluating electric vehicle charging impacts and customer charging behaviors-experience from six smart grid investment grant projects, office of electricity delivery and energy reliability, us department of energy," 2014.

[28] P. O. of the European Union. (2013) Projections for Electric Vehicle Load Profiles in Europe Based on Travel Survey Data. https://publications.jrc.ec.europa.eu/repository/handle/JRC82307. Accessed: 2023-12-25.

[29] X. Energy, "Electric vehicle charging station: pilot evaluation report," *Xcel Energy, Colorado*, 2015.

[30] M. Kamruzzaman and M. Benidris, "Modeling of electric vehicles as movable loads in composite system reliability assessment," in *2018 IEEE Power Energy Society General Meeting (PESGM)*, 2018, pp. 1–5.

[31] M. Benidris and J. Mitra, "Reliability and sensitivity analysis of composite power systems under emission constraints," *IEEE Transactions on Power Systems*, vol. 29, no. 1, pp. 404–412, 2013.

[32] C. Singh and J. Mitra, "Reliability analysis of emergency and standby power systems," *IEEE Industry Applications Magazine*, vol. 3, no. 5, pp. 41–47, 1997.

[33] C. Singh, P. Jirutitijaroen, and J. Mitra, *Electric power grid reliability evaluation: models and methods*. John Wiley & Sons, 2018.

[34] P. M. Subcommittee, "Ieee reliability test system," *IEEE Transactions on Power Apparatus and Systems*, vol. PAS-98, no. 6, pp. 2047–2054, 1979.